Monitoring Orientation and Dynamics of Membrane-Bound Melittin Utilizing Dansyl Fluorescence

Sourav Haldar, H. Raghuraman,† and Amitabha Chattopadhyay*

Centre for Cellular and Molecular Biology, Council of Scientific and Industrial Research, Uppal Road, Hyderabad 500 007, India

Received: June 16, 2008; Revised Manuscript Received: August 26, 2008

Melittin is a cationic hemolytic peptide isolated from the European honey bee, *Apis mellifera*. In spite of a number of studies, there is no consensus regarding the orientation of melittin in membranes. In this study, we used a melittin analogue that is covalently labeled at its amino terminal (Gly-1) with the environment-sensitive 1-dimethylamino-5-sulfonylnaphthalene (dansyl) group to obtain information regarding the orientation and dynamics of the amino terminal region of membrane-bound melittin. Our results show that the dansyl group in Dns-melittin exhibits red edge excitation shift in vesicles of 1,2-dioleoyl-*sn*-glycero-3-phosphocholine, implying its localization in a motionally restricted region of the membrane. This is further supported by wavelength-dependent anisotropy and lifetime changes and time-resolved emission spectra characterized by dynamic Stokes shift, which indicates relatively slow solvent relaxation in the excited state. Membrane penetration depth analysis using the parallax method shows that the dansyl group is localized at a depth of ~18 Å from the center of the bilayer in membrane-bound Dns-melittin. Further analysis of dansyl and tryptophan depths in Dns-melittin shows that the tilt angle between the helix axis of membrane-bound melittin and the bilayer normal is ~70°. Our results therefore suggest that melittin adopts a pseudoparallel orientation in DOPC membranes at low concentration.

Introduction

Melittin, the principal toxic component in the venom of the European honey bee, *Apis mellifera*, is a cationic hemolytic peptide.[1] It is a small linear peptide composed of 26 amino acids (NH_2-GIGAVLKVLTTGLPALISWIKRKRQQ-$CONH_2$) in which the amino-terminal region (residues 1−20) is predominantly hydrophobic whereas the carboxy-terminal region (residues 21−26) is hydrophilic due to the presence of a stretch of positively charged amino acids. This amphiphilic property of melittin makes it water soluble and yet it spontaneously associates with natural and artificial membranes.[2,3] Such a sequence of amino acids, coupled with its amphiphilic nature, is characteristic of many membrane-bound peptides and putative transmembrane helices of membrane proteins.[2,4] This has resulted in melittin being used as a convenient model for monitoring lipid−protein interactions in membranes.[3]

Melittin adopts predominantly random coil conformation as a monomer in aqueous solution.[5] However, at high ionic strength, pH, or peptide concentration, it self-associates to form an α-helical tetrameric structure driven by the formation of a hydrophobic core.[2,3,5,6] Interestingly, melittin adopts an α-helical conformation when bound to membranes of varying lipid composition[2,3,7−10] or micellar systems.[11,12] Despite the availability of a high resolution crystal structure of tetrameric melittin in aqueous solution,[13] the structure of the membrane-bound form is not yet resolved by X-ray crystallography. Yet, the importance of the membrane-bound form stems from the observation that the amphiphilic α-helical conformation of this hemolytic toxin in membranes resembles those of apolipoproteins and peptide hormones,[14] signal peptides,[15] and the envelope glycoprotein gp41 from the human immunodeficiency virus (HIV).[16] Furthermore, understanding melittin-membrane interaction assumes greater significance due to the observation that melittin mimics the amino terminal of HIV-1 virulence factor Nef1−25.[17]

Melittin is intrinsically fluorescent due to the presence of a single tryptophan residue, Trp-19, in the carboxy terminal region which has been extensively utilized as a sensitive probe to monitor the interaction of melittin with membranes and membrane-mimetic systems by us[8−12] and other groups.[18−20] We have previously monitored the microenvironment experienced by the sole tryptophan in membrane-bound melittin and its modulation by anionic phospholipids, cholesterol, unsaturation, and ionic strength utilizing the wavelength-selective fluorescence approach.[8−10,21] We showed that the tryptophan residue is located in a motionally restricted interfacial region of the membrane in all cases. However, a limitation of utilizing tryptophan fluorescence is that the information essentially comes only from the carboxy terminal region of melittin, and information about the amino terminal region is only beginning to be addressed.[22] The lack of information about the amino terminal region of melittin makes it difficult to comment about the orientation of melittin in membranes.

In this paper, we used a melittin analogue that is covalently labeled at its amino terminal (Gly-1) with an environment-sensitive fluorescent group 1-dimethylamino-5-sulfonylnaphthalene (dansyl) (see inset in Figure 1) to obtain information regarding the orientation and dynamics of the amino terminal region of membrane-bound melittin utilizing dansyl fluorescence. The dansyl group is extensively used to fluorescently label proteins, peptides, and lipids due to the environmental sensitivity of its fluorescence and favorable lifetime.[23] An advantage of using dansylated peptides and proteins is that

* To whom correspondence should be addressed. Tel.: +91-40-2719-2578. Fax: +91-40-2716-0311. E-mail: amit@ccmb.res.in.

† Present address: Department of Biochemistry and Molecular Biology, The University of Chicago, Center for Integrative Sciences, 929 East 57th Street, Chicago, IL 60637.

10.1021/jp805299g CCC: $40.75 © 2008 American Chemical Society
Published on Web 10/09/2008

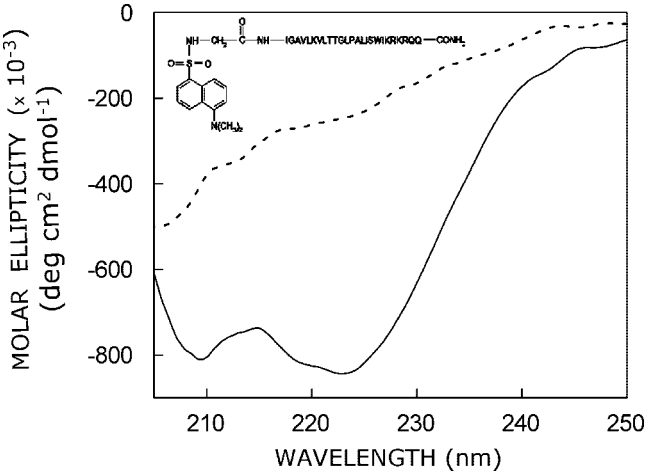

Figure 1. Representative far-UV CD spectra of Dns-melittin in water (---) and bound to DOPC vesicles (——). The ratio of Dns-melittin/DOPC was 1:100 (mol/mol) and the concentration of Dns-melittin was 17 μM in both cases. See Experimental Section for other details. The chemical structure of Dns-melittin is shown in the inset.

proteins do not absorb in the wavelength range where the dansyl group is excited. The dansyl group exhibits a relatively large Stokes shift and its emission spectrum is highly sensitive to environmental polarity. Since the sole tryptophan is located at the carboxy terminal region of melittin, the information obtained from Dns-melittin fluorescence would provide an additional convenient tool to monitor the conformation and dynamics of membrane-bound melittin. We report here that the dansyl group in membrane-bound Dns-melittin exhibits red edge excitation shift (REES) indicating slow dielectric relaxation in its immediate environment due to motional restriction at the membrane interface. This is further supported by time-resolved fluorescence measurements and time-resolved emission spectra which show dynamic Stokes shift. Overall, our results suggest that the orientation of melittin is pseudoparallel to the plane of the membrane surface, and we provide an estimate of the tilt angle to the bilayer normal from analysis of membrane penetration depths.

Experimental Section

Materials. 1,2-dimyristoyl-*sn*-glycero-3-phosphocholine (DMPC) and 3-(*N*-morpholino) propanesulfonic acid (MOPS) were obtained from Sigma Chemical Co. (St. Louis, MO). 1, 2-dioleoyl-*sn*-glycero-3-phosphocholine (DOPC), 1,2-dioleoyl-*sn*-glycero-3-phosphotempocholine (Tempo-PC), 1-palmitoyl-2-(5-doxyl)stearoyl-*sn*-glycero-3-phosphocholine (5-PC), and 1-palmitoyl-2-(12-doxyl)stearoyl-*sn*-glycero-3-phosphocholine (12-PC), were purchased from Avanti Polar Lipids (Alabaster, AL). Anthroyloxy-labeled fatty acids such as 2-(9-anthroyloxy) stearic acid (2-AS) and 12-(9-anthroyloxy) stearic acid (12-AS) were from Molecular Probes (Eugene, OR). Dansyl-labeled melittin (Dns-melittin) was custom synthesized by Mimotopes (Clayton, Australia). Initial experiments were performed with an aliquot of Dns-melittin kindly provided by Dr. Franklyn Prendergast (Mayo Clinic, Rochester, MN). Lipids were checked for purity by thin layer chromatography on silica gel precoated plates (Sigma) in chloroform/methanol/water (65:35:5, v/v/v) and were found to give only one spot in all cases with a phosphate-sensitive spray and on subsequent charring.[24] The concentration of DOPC was determined by phosphate assay subsequent to total digestion by perchloric acid.[25] DMPC was used as an internal standard to assess lipid digestion. The concentration of Dns-melittin in aqueous solution was calculated from the absorbance values at 330 nm with the contribution of the dansyl group at 330 nm added to the absorbance due to the tryptophan side chain, using a resultant molar extinction coefficient (ε) of 5220 M^{-1} cm^{-1}. All other chemicals used were of the highest purity available. The solvents used were of spectroscopic grade. Water was purified through a Millipore (Bedford, MA) Milli-Q system and used throughout.

Sample Preparation. All experiments were done using large unilamellar vesicles (LUVs) of 100 nm diameter containing 1 mol% Dns-melittin. In general, 640 nmol of DOPC was dried under a stream of nitrogen while being warmed gently (~35 °C). After further drying under a high vacuum for more than 3 h, 1.5 mL of 10 mM MOPS, 150 mM NaCl, pH 7.2 buffer was added, and the sample was vortexed for 3 min to disperse the lipid and form homogeneous multilamellar vesicles. LUVs of 100 nm diameter were prepared by the extrusion technique using an Avestin Liposofast Extruder (Ottawa, Ontario, Canada) as previously described.[26] Briefly, the multilamellar vesicles were freeze-thawed five times using liquid nitrogen to ensure solute equilibration between trapped and bulk solutions and then extruded through polycarbonate filters (pore diameter of 100 nm) mounted in the extruder fitted with Hamilton syringes (Hamilton Company, Reno, NV). The samples were subjected to 11 passes through polycarbonate filters to give the final LUV suspension. To incorporate Dns-melittin into membranes, a small aliquot containing 6.4 nmol of Dns-melittin was added from a stock solution in water to the preformed vesicles and mixed well. The samples were incubated in dark for 12 h at room temperature (~23 °C) for equilibration before making measurements. Background samples were prepared the same way except that Dns-melittin was not added to them. All experiments were performed at room temperature (~23 °C).

Depth Measurements Using the Parallax Method. The actual spin (nitroxide) content of the spin-labeled phospholipids (Tempo- and 5-PC) was assayed using fluorescence quenching of anthroyloxy-labeled fatty acids (2- and 12-AS) as described earlier.[27] For depth measurements, liposomes were made by the ethanol injection method.[28] These samples were made by drying 160 nmol of DOPC containing 10 mol% spin-labeled phospholipid (Tempo- or 5-PC) under a stream of nitrogen while being warmed gently (~35 °C) followed by further drying under a high vacuum for at least 3 h. The dried lipid film was dissolved in ethanol to give a final concentration of 40 mM. The ethanolic lipid solution was then injected into 10 mM MOPS, 150 mM NaCl, pH 7.2 buffer, while vortexing to give a final concentration of 0.11 mM DOPC in buffer. Dns-melittin was incorporated into membranes by adding a small aliquot containing 1.6 nmol of peptide from a stock solution in water to the preformed vesicles and mixed well to give membranes containing 1% Dns-melittin. The lipid composition of these samples was DOPC (90%) and Tempo- (or 5-PC) (10%). Duplicate samples were prepared in each case except for samples lacking the quencher (Tempo- or 5-PC) where triplicates were prepared. Background samples lacking the fluorophore (Dns-melittin) were prepared in all cases, and their fluorescence intensity was subtracted from the respective sample fluorescence intensity. Samples were kept in the dark for 12 h before measuring fluorescence.

Steady State Fluorescence Measurements. Steady state fluorescence measurements were performed with a Hitachi F-4010 spectrofluorometer using 1 cm path length quartz cuvettes. Excitation and emission slits with a nominal bandpass of 5 nm were used for all measurements. Background intensities of samples in which Dns-melittin was omitted were subtracted

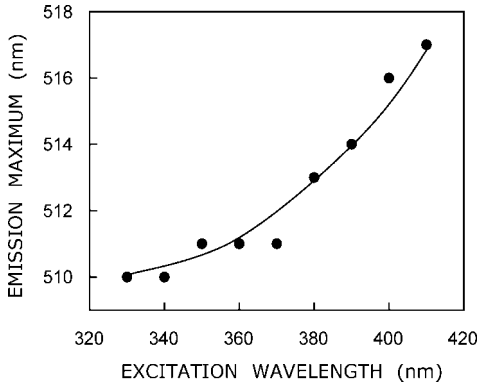

Figure 2. Effect of changing excitation wavelength on the wavelength of maximum emission of Dns-melittin bound to vesicles made of DOPC. The ratio of Dns-melittin/DOPC was 1:100 (mol/mol) and the concentration of Dns-melittin was 4.27 μM. The line joining the data points is provided merely as a viewing guide. See Experimental Section for other details.

from each sample spectrum to cancel out any contribution due to the solvent Raman peak and other scattering artifacts. The spectral shifts obtained with different sets of samples were identical in most cases. In other cases, the values were within $\pm$1 nm of the ones reported. Fluorescence anisotropy measurements were performed at room temperature ($\sim$23 °C) using a Hitachi polarization accessory. Anisotropy values were calculated from the equation:[23]

$$r = \frac{I_{VV} - GI_{VH}}{I_{VV} + 2GI_{VH}} \quad (1)$$

where I_{VV} and I_{VH} are the measured fluorescence intensities (after appropriate background subtraction) with the excitation polarizer oriented vertically and the emission polarizer vertically and horizontally oriented, respectively. G is the grating correction factor and is the ratio of the efficiencies of the detection system for vertically and horizontally polarized light and is equal to I_{HV}/I_{HH}. All experiments were done with multiple sets of samples and average values of anisotropy are shown in Figure 3.

For depth measurements, samples were excited at 330 nm and emission was collected at 512 nm. Excitation and emission slits with a nominal bandpass of 5 nm were used. Fluorescence was measured at room temperature ($\sim$23 °C) and averaged over two 5 s readings. Intensities were found to be stable over time. In all cases, the intensity from background samples without fluorophore (Dns-melittin) was subtracted. Membrane penetration depths were calculated using eq 5 (see Results).

Time-Resolved Fluorescence Measurements. Fluorescence lifetimes were calculated from time-resolved fluorescence intensity decays using IBH 5000F NanoLED equipment (Horiba Jobin Yvon, Edison, NJ) with DataStation software in the time-correlated single photon counting mode. A pulsed light-emitting diode (LED) (NanoLED-16) was used as an excitation source. This LED generates optical pulse at 337 nm of pulse duration 1.2 ns and is run at 1 MHz repetition rate. LED profile (instrument response function) was measured at the excitation wavelength using Ludox (colloidal silica) as the scatterer. To optimize the signal-to-noise ratio, 10 000 photon counts were collected in the peak channel. All experiments were performed using emission slits with a bandpass of 4 nm or less. The sample and the scatterer were alternated after every 5% acquisition to ensure compensation for shape and timing drifts occurring during the period of data collection. This arrangement also prevents any prolonged exposure of the sample to the excitation beam thereby avoiding any possible photodamage of the fluorophore. The data was stored and analyzed using DAS 6.2 software (Horiba Jobin Yvon, Edison, NJ). Fluorescence intensity decay curves so obtained were deconvoluted with the instrument response function and analyzed as a sum of exponential terms

$$F(t) = \Sigma_i \alpha_i \exp(-t/\tau_i) \quad (2)$$

where $F(t)$ is the fluorescence intensity at time t and α_i is a pre-exponential factor representing the fractional contribution to the time-resolved decay of the component with a lifetime τ_i such that $\Sigma_i \alpha_i = 1$. The program also includes statistical and plotting subroutine packages.[29] The goodness of the fit of a given set of observed data and the chosen function was evaluated by the χ^2 ratio, the weighted residuals,[30] and the autocorrelation function of the weighted residuals.[31] A fit was considered acceptable when plots of the weighted residuals and the autocorrelation function showed random deviation about zero with a minimum χ^2 value not more than 1.4. Intensity-averaged mean lifetimes $\langle\tau\rangle$ for biexponential decays of fluorescence were calculated from the decay times and pre-exponential factors using the following equation:[23]

$$\langle\tau\rangle = \frac{\alpha_1\tau_1^2 + \alpha_2\tau_2^2}{\alpha_1\tau_1 + \alpha_2\tau_2} \quad (3)$$

In order to obtain time-resolved emission spectra (TRES), a series of fluorescence decays were acquired over a range of emission wavelengths (480−520 nm) across the emission spectrum, using a constant excitation wavelength of 337 nm. All the decay curves were then individually fitted as a sum of exponential terms as discussed above. The net result of such an analysis was a set of deconvoluted intensity decays at various emission wavelengths, that is, a three-dimensional data set of counts versus time versus emission wavelength. This three-dimensional data set is then sliced orthogonally to the time axis to produce two-dimensional spectra of counts versus emission wavelength in order to visualize how the emission spectrum evolves during the fluorescence lifetime. This method has the advantage that convolution distortion is avoided because each decay curve is individually deconvoluted before the construction of the final TRES plot.

Circular Dichroism Measurements. CD measurements were carried out at room temperature ($\sim$23 °C) on a JASCO J-715 spectropolarimeter which was calibrated with (+)−10-camphorsulfonic acid. The spectra were scanned in a quartz optical cell with a path length of 0.1 cm. Spectra were recorded in 0.2 nm wavelength increments with a 4 s response and a bandwidth of 1 nm. For monitoring changes in secondary structure, spectra were scanned in the far-UV range from 205 to 250 nm at a scan rate of 50 nm/min. Each spectrum is the average of 15 scans with a full scale sensitivity of 50 mdeg. Spectra were corrected for background by subtraction of appropriate blanks and were smoothed making sure that the overall shape of the spectrum remains unaltered. Data are represented as molar ellipticities and were calculated using the equation

$$[\theta] = \theta_{obs}/(10Cl) \quad (4)$$

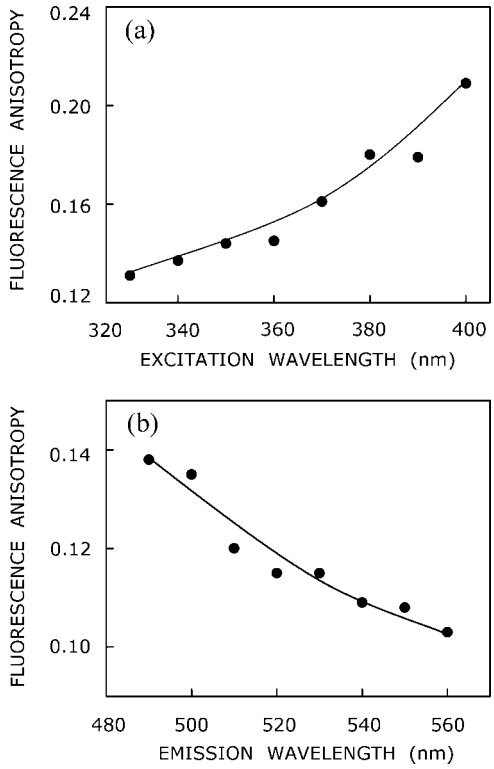

Figure 3. Fluorescence anisotropy of Dns-melittin in DOPC membranes as a function of (a) excitation and (b) emission wavelengths. The anisotropy values were recorded at an emission wavelength of 512 nm (panel a), and the excitation wavelength used was 330 nm (panel b). Data shown are means of three independent measurements. All other conditions are as in Figure 2. The lines joining the data points are provided merely as viewing guides. See Experimental Section for other details.

where θ_{obs} is the observed ellipticity in mdeg, l is the path length in cm, and C is the concentration of melittin analogue in mol/L.

Results

It is well established that monomeric melittin in aqueous solution shows essentially random coil conformation as reported earlier.[8,9] On the other hand, membrane-bound melittin shows a CD spectrum which is characteristic of an α-helical conformation.[7−10,32,33] To examine the secondary structural characteristics of Dns-melittin, we carried out far-UV CD spectroscopy of Dns-melittin. The CD spectra of Dns-melittin in water and when bound to DOPC vesicles are shown in Figure 1. Dns-melittin in water shows essentially random secondary structure. The CD spectrum in DOPC membranes show that the secondary structure of membrane-bound Dns-melittin is α-helical and does not appear to be affected by the presence of the dansyl group.

REES represents a powerful approach which can be used to directly monitor the environment and dynamics around a fluorophore in a complex biological system.[34−36] A shift in the wavelength of maximum fluorescence emission toward higher wavelengths, caused by a shift in the excitation wavelength toward the red edge of the absorption band, is termed REES. This effect is mostly observed with polar fluorophores in motionally restricted environments where the dipolar relaxation time for the solvent shell around a fluorophore is comparable to or longer than its fluorescence lifetime. REES arises from slow rates of solvent relaxation (reorientation) around an excited-state fluorophore which depends on the motional restriction imposed on the solvent molecules in the immediate vicinity of the fluorophore. This is particularly relevant in the case of organized molecular assemblies such as membranes (liposomes) where slower solvent dynamics has been earlier reported due to constrained environment.[37,38] Utilizing this approach, it becomes possible to probe the mobility parameters of the environment itself, represented by the relaxing solvent molecules or the dipolar environment,[39,40] using the fluorophore merely as a reporter group. While other fluorescence techniques yield information about the fluorophore itself, REES provides information about the relative rates of solvent relaxation which is not possible to obtain by other techniques. Since the dynamics of hydration is directly associated with the functionality of proteins, REES has proved to be a useful tool to explore the organization and dynamics of soluble and membrane proteins under varying degrees of hydration.[11,40] REES serves as a powerful tool to monitor the organization and dynamics of melittin bound to membranes and membrane-mimetic environments.[8,11,12]

The fluorescence emission maximum of Dns-melittin in DOPC membranes is 510 nm, when excited at 330 nm (see Figure 2). The shift in the maxima of fluorescence emission[41] of the dansyl group of Dns-melittin when bound to DOPC vesicles as a function of excitation wavelength is shown in Figure 2. As the excitation wavelength is changed from 330 to 410 nm, the emission maximum of membrane-bound Dns-melittin is shifted from 510 to 517 nm which corresponds to REES of 7 nm. Such dependence of the emission maximum on excitation wavelength is characteristic of REES. This implies that the dansyl group of Dns-melittin is localized in a motionally restricted region of the membrane. This is consistent with the interfacial localization of the melittin when bound to membranes.[8,9,42] The membrane interface is characterized by unique motional and dielectric characteristics distinct from both the bulk aqueous phase and the more isotropic hydrocarbon-like deeper regions of the membrane.[34,43] This specific region of the membrane exhibits slow rates of solvent relaxation and is also known to participate in intermolecular charge interactions and hydrogen bonding through the polar headgroup. These structural features, which slow down the rate of solvent reorientation, have previously been recognized as typical features of microenvironments giving rise to significant REES. It is therefore the membrane interface which is most likely to display red edge effects.[34]

Fluorescence anisotropy is known to be dependent on excitation and emission wavelengths in motionally restricted media.[44] The change in anisotropy of Dns-melittin in DOPC membranes as a function of excitation and emission wavelengths is shown in Figure 3. The figure shows that membrane-bound Dns-melittin exhibits wavelength-dependent changes in anisotropy for both excitation (Figure 3a) and emission (Figure 3b) wavelengths. This reinforces our previous conclusion that Dns-melittin is localized in a motionally restricted interfacial region of the membrane in these cases (see results of depth analysis below).

Fluorescence lifetime serves as a faithful indicator of the local environment in which a given fluorophore is placed.[45] In addition, it is well known that fluorescence lifetime of the dansyl moiety is sensitive to its local environment.[46−48] A typical decay profile of Dns-melittin in DOPC membranes with its biexponential fitting and the statistical parameters used to check the goodness of the fit is shown in Figure 4. The fluorescence lifetimes of Dns-melittin in buffer and bound to DOPC membranes are shown in Table 1. As seen from the table, both the fluorescence decays could be fitted well with a biexponential

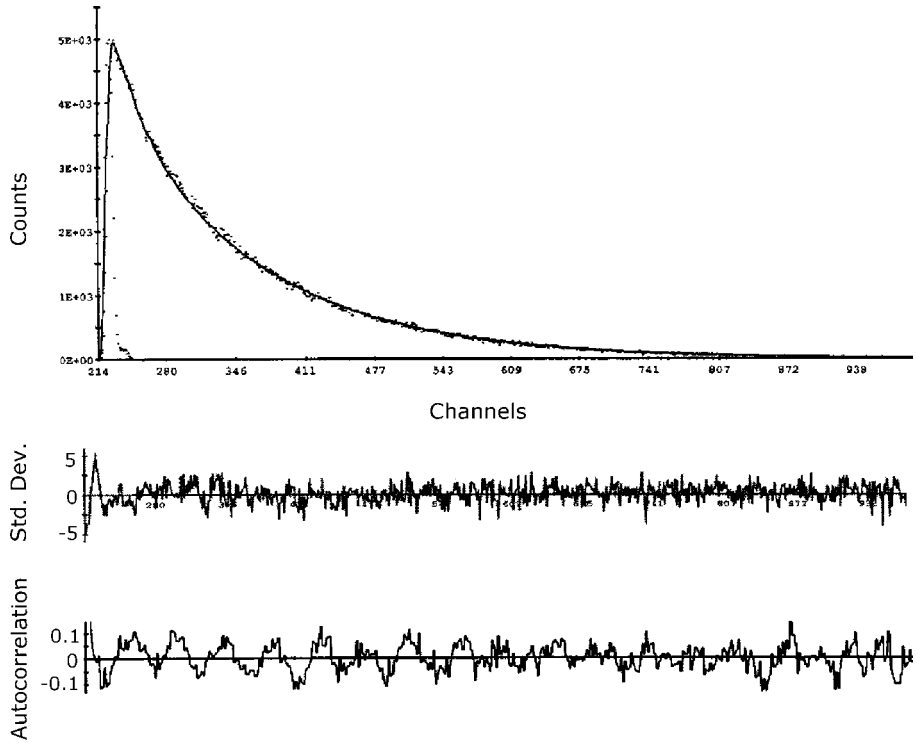

Figure 4. Time-resolved fluorescence intensity decay of Dns-melittin in DOPC membranes. Excitation wavelength was 337 nm corresponding to pulsed diode light source and emission was monitored at 512 nm. The sharp peak on the left corresponds to the profile of the pulsed light emitting diode (LED). The relatively broad peak on the right is the decay profile, fitted to a biexponential function. The two lower plots show the weighted residuals and the autocorrelation function of the weighted residuals. All other conditions are as in Figure 2. See Experimental Section for other details.

TABLE 1: Fluorescence Lifetimes of Dns-Melittin[a]

condition	α_1	τ_1 (ns)	α_2	τ_2 (ns)	$\langle\tau\rangle$ (ns)
Buffer	0.58	3.35	0.42	13.94	11.90
DOPC membranes	0.15	5.15	0.85	15.98	15.39

[a] The excitation wavelength was 337 nm; emission was monitored at 540 and 512 nm in buffer and DOPC membranes, respectively. The number of photons collected at the peak channel was 10 000. See Experimental Section for other details.

TABLE 2: Fluorescence Lifetimes of Membrane-Bound Dns-Melittin As a Function of Emission Wavelength[a]

emission wavelength (nm)	α_1	τ_1 (ns)	α_2	τ_2 (ns)
510	0.07	3.32	0.93	14.96
520	0.03	1.94	0.97	15.27
530	0.05	7.53	0.95	15.67
540	−0.01	7.59	1.01	15.45
560	−0.09	5.43	1.09	15.65

[a] The excitation wavelength was 337 nm. The number of photons collected at the peak channel was 10 000. See Experimental Section for other details.

function. The mean fluorescence lifetime, calculated from Table 1 using eq 3, for Dns-melittin in buffer is 11.90 ns (Table 1). The mean fluorescence lifetime of Dns-melittin in DOPC membranes is increased to 15.39 ns due to a change in apparent polarity experienced by the fluorophore. We chose to use the mean fluorescence lifetime as an important parameter since it is independent of the number of exponentials used to fit the time-resolved fluorescence decay.

The fluorescence lifetimes of Dns-melittin in DOPC membranes as a function of emission wavelength are shown in Table 2. All fluorescence decays could be fitted well with a biexponential function. Interestingly, when the fluorescence decays were analyzed toward the red edge of emission (>530 nm), a component with negative pre-exponential factor is required to fit the data. This suggests that emission at these wavelengths is contributed from intermediates created in the excited-state due to slow solvent relaxation (see also Figure 5). Such negative pre-exponential factor has earlier been reported for the decay of the dansyl group in restricted environments.[46,48] The mean fluorescence lifetime of Dns-melittin in DOPC membranes are plotted as a function of emission wavelength in Figure 5. Interestingly, the mean fluorescence lifetime displays a considerable increase with increasing emission wavelength from 510 to 560 nm. Similar observation of increasing lifetime with increasing emission wavelength has previously been reported for fluorophores in environments of restricted mobilities.[44] Such increasing lifetimes across the emission spectrum may be interpreted in terms of solvent reorientation around the excited-state fluorophore as follows. Observation of emission spectra at shorter wavelengths selects for predominantly unrelaxed fluorophores. Their lifetimes are shorter because this population is decaying both at the rate of fluorescence emission at the given excitation wavelength and by decay to longer (unobserved) wavelengths. In contrast, observation at the long wavelength (red edge) of the emission selects for the more relaxed fluorophores, which have spent enough time in the excited-state to allow increasingly larger extents of solvent relaxations. These longer-lived fluorophores, which emit at higher wavelengths, should have more time to rotate in the excited state, giving rise to lower anisotropy. As already seen (Figure 3b), there is considerable decrease in anisotropy of Dns-melittin in DOPC membranes with increasing emission wavelength. The lowest anisotropy is observed toward longer wavelengths (red edge) where emission from the relaxed fluorophores predominates.

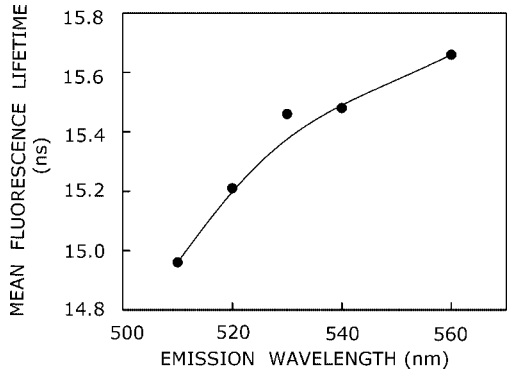

Figure 5. Mean fluorescence lifetime of Dns-melittin in DOPC membranes as a function of emission wavelength. Excitation wavelength used was 337 nm. Mean fluorescence lifetimes were calculated from Table 2 using eq 3. All other conditions are as in Figure 2. See Experimental Section for other details.

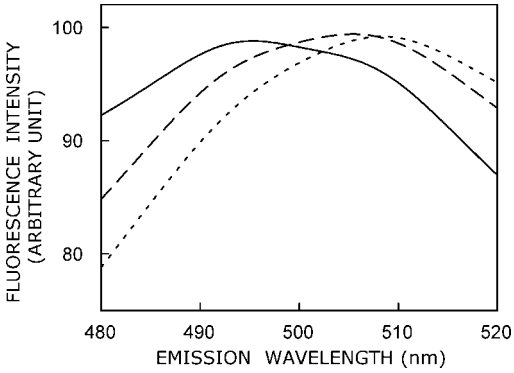

Figure 6. TRES of Dns-melittin in DOPC membranes reconstructed from fluorescence decays measured at different emission wavelengths across the emission spectrum. The emission spectra correspond to early ((—), up to 4 ns after excitation), intermediate ((- - -), up to 15 ns after excitation) and late ((•••••), up to 30 ns after excitation) time points. Spectra acquired at early, intermediate, and late time points correspond to initial (unrelaxed) excited state, partially relaxed state, and fully relaxed state. The emission maximum gradually moves toward the red edge of the spectrum with time. All spectra are intensity-normalized at the emission maximum. Excitation wavelength used was 337 nm. All other conditions are as in Figure 2. See Experimental Section for other details.

TABLE 3: Penetration Depth of the Membrane-Bound Dns-Melittin by the Parallax Method

fluorophore	distance from the center of the bilayer, z_{cF} (Å)[a]
dansyl group at the amino terminal	18.0
tryptophan-19	10.6[b]

[a] Depths were calculated from fluorescence quenchings obtained with samples containing 10 mol % of Tempo-PC and 5-PC and using eq 5. Samples were excited at 330 nm, and emission was collected at 512 nm. The ratio of Dns-melittin to total lipid was 1:100 (mol/mol) and the concentration of Dns-melittin was 1.07 μM in all cases. See Experimental Section for other details. [b] From ref 8.

Figure 6 shows the time-resolved emission spectra (TRES) of Dns-melittin in DOPC membranes at early (up to 4 ns after excitation), intermediate (up to 15 ns after excitation), and late (up to 30 ns after excitation) time points. The figure shows that there is a progressive red shift in the emission spectrum with time. For the early time point spectrum, the emission maximum is at ~495 nm, while it progressively shifts to ~504 and ~510 nm for intermediate and late time points. This dynamic change in emission maximum indicates (i.e., changes in the emission spectra occurring during the fluorescence lifetime) relatively slow solvent relaxation in the excited state (which also gives rise to REES).

Membrane penetration depth represents an important parameter in the study of membrane structure and organization.[49,50] Knowledge of the precise depth of a membrane embedded group or molecule often helps define the conformation and topology of membrane probes and proteins. In order to gain an overall understanding of the organization and conformation of the amino terminal region of membrane-bound melittin, penetration depths of the dansyl group of Dns-melittin in DOPC membranes was determined. Depth of the dansyl group was calculated by the parallax method[51] using the equation

$$z_{cF} = L_{c1} + \{[(-1/\pi C)\ln(F_1/F_2) - L_{21}^2]/2L_{21}\} \quad (5)$$

where z_{cF} is the depth of the fluorophore from the center of the bilayer, L_{c1} is the distance of the center of the bilayer from the shallow quencher (Tempo-PC in this case), L_{21} is the difference in depth between the two quenchers (i.e., the transverse distance between the shallow and the deep quencher), and C = the two-dimensional quencher concentration in the plane of the membrane (molecules/Å^2). Here F_1/F_2 is the ratio of F_1/F_o and F_2/F_o in which F_1 and F_2 are fluorescence intensities in the presence of the shallow (Tempo-PC) and deep quencher (5-PC), respectively, both at the same quencher concentration C; F_o is the fluorescence intensity in the absence of any quencher. All the bilayer parameters used were the same as described previously.[51] The depth of penetration of the dansyl group of Dns-melittin bound DOPC membranes is shown in Table 3. The depth of penetration of the tryptophan residue of native melittin in these membranes is provided in the table for comparison. Our results show that the depth of penetration of the dansyl group of Dns-melittin is found to be, on an average, ~18 Å from the center of the bilayer (see Figure 7). This suggests that Gly-1 of melittin is located at a relatively shallow interfacial region of the membrane (near headgroups). We have previously shown that the tryptophan residue (Trp-19) of native melittin is located at a deeper interfacial region (near the carbonyl group, 10.6 Å from the center of the bilayer) in DOPC membranes[8,9] (see Figure 7).

Discussion

As mentioned earlier, a large body of literature exists on melittin-membrane interaction using tryptophan fluorescence. Since fluorescence spectroscopic approaches provide information on a local scale and the sole tryptophan residue in melittin is localized in the carboxy terminal region of melittin, very little is known about the orientation and dynamics in the amino terminal region. In this work, we have monitored the organization and dynamics of Dns-melittin bound to DOPC membranes in order to obtain information about the location and dynamics of the amino terminal region of membrane-bound melittin. This was achieved by covalently labeling the amino terminal end of melittin with the environment-sensitive fluorescent dansyl group. Our results show that the dansyl group in membrane-bound Dns-melittin exhibits REES implying its localization in a motionally restricted region of the membrane. An important criterion for a fluorophore to exhibit REES is a relatively large change in dipole moment upon excitation.[34,35] The dansyl group is particularly suitable in this respect since it has been earlier shown that it undergoes a large dipole moment change upon excitation.[52] The motionally restricted environment of the dansyl group in the

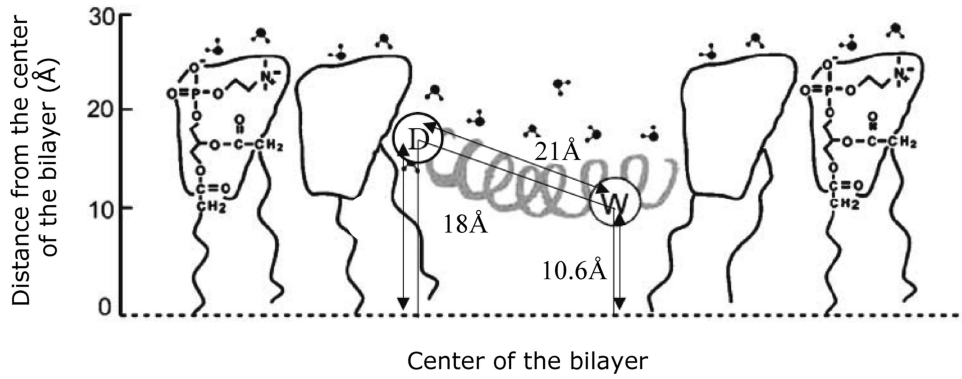

Figure 7. A schematic representation of the membrane bilayer showing the orientation and location of fluorescent groups in membrane-bound Dns-melittin. The small v-shaped structures represent membrane associated water molecules. The sole tryptophan residue (W) and the dansyl group (D) of membrane-bound Dns-melittin are shown to be localized in the interfacial region of membranes. Membrane penetration depths of tryptophan (10.6 Å from the center of the bilayer) and the dansyl group (18 Å) of membrane-bound Dns-melittin (see Table 3) along with the distance between the tryptophan and the dansyl group (21 Å, from ref 53) allow us to calculate the angle between the helix axis of melittin and the bilayer normal. The dotted line indicates the center of the bilayer. See text for other details. Adapted and modified from ref 9.

membrane is further supported by wavelength-dependent anisotropy and lifetime changes, and time-resolved emission spectra characterized by dynamic Stokes shift, which indicates relatively slow solvent relaxation in the excited state.

Figure 7 shows the orientation of Dns-melittin and the location (depth) of the dansyl group and tryptophan in DOPC membranes. Membrane penetration depth analysis using the parallax method shows that the depth of penetration of the dansyl group of Dns-melittin is ~18 Å from the center of the bilayer (see Table 3). This is in excellent agreement with our previous results of depth analysis, using melittin labeled with the NBD group at its amino terminal.[22] Taken together, these data imply that the amino terminal end of melittin is located at a relatively shallow interfacial region of the membrane, possibly toward the headgroup region. Interestingly, we have previously shown that the tryptophan residue (Trp-19) of melittin at the carboxy terminal, is located at a deeper interfacial region (near the carbonyl group) at ~10.6 Å from the center of the bilayer in DOPC membranes [8,9] (see Table 3). Knowledge of penetration depths of these two fluorophores on membrane-bound Dns-melittin helps us to comment on the orientation of melittin in the membrane. Different depths obtained for the dansyl group and tryptophan suggest that the helix axis of membrane-bound melittin is possibly not parallel to the membrane surface. In other words, membrane-bound melittin adopts a pseudoparallel orientation with a tilt angle. The distance between the dansyl group and tryptophan in membrane-bound Dns-melittin has previously been reported to be ~21 Å from energy transfer measurements.[53] This distance, along with the penetration depths of the dansyl group and tryptophan, allow us to calculate the tilt angle between the helix axis of membrane-bound melittin and the bilayer normal from simple geometric considerations. When calculated this way, the angle between the helix axis of membrane-bound Dns-melittin and the bilayer normal is found to be [$90° - \sin^{-1}$ (7.4/21)], which turns out to be ~70°. Our data therefore suggest that melittin adopts a pseudoparallel orientation in DOPC membranes at low concentrations. Interestingly, the tilt angle of membrane-bound melittin calculated this way is in good agreement with the tilt angle predicted from energetics considerations in a recent theoretical study.[54]

Despite a number of studies addressed to determine the orientation (parallel or perpendicular) of membrane-bound melittin with respect to the plane of the membrane bilayer,[2,3,32,42,55−57] there is no consensus regarding the orientation of melittin in membranes. This is due to the fact that the orientation of melittin in membranes is critically dependent on the peptide concentration, membrane lipid composition, and membrane properties which include hydration and the phase state of the lipid.[32] For example, it has been shown that the orientation of membrane-bound melittin depends on temperature, and melittin adopts perpendicular orientation in fluid phase DMPC,[32,58] DLPC, and DTPC membranes.[32] In contrast, melittin orients parallel to the membrane surface in DOPC[42] and DPhPC[32] membranes in which there is very little dependence on temperature. Interestingly, the orientation of melittin in POPC membranes is complicated since it assumes parallel or perpendicular orientation depending upon the peptide concentration, though these membranes are in the fluid phase.[32] In addition, the orientation of membrane-bound melittin is further complicated by the observation that melittin does not adopt a fully transmembrane orientation in membranes, but a pseudotransmembrane orientation.[55,56,59] We show here, by analysis of membrane penetration depths of Dns-melittin in DOPC membranes at low concentrations, that melittin adopts a pseudoparallel orientation. These results are in agreement with previous reports that show that membrane-bound melittin orients parallel to the membrane plane[2,32,42,60] and with the hypothesis that transmembrane orientation may not be an absolute requirement for the lytic activity of cationic, amphipathic peptides (i.e., "carpetlike"model).[4,20,61]

Acknowledgment. This work was supported by the Council of Scientific and Industrial Research, Government of India. S.H. and H.R. thank the Council of Scientific and Industrial Research, Government of India, for the award of Junior Research Fellowship and Research Associateship. A.C. is an Adjunct Professor at the Special Centre for Molecular Medicine of Jawaharlal Nehru University (New Delhi, India) and Honorary Professor of the Jawaharlal Nehru Centre for Advanced Scientific Research, (Bangalore, India). We thank Phyllis Fisher (Mayo Clinic, Rochester, MN), Sandeep Shrivastava, Lora B. Narayana, and G.G. Kingi for technical help and members of our laboratory for critically reading the manuscript.

References and Notes

(1) Habermann, E. *Science* **1972**, *177*, 314.
(2) Dempsey, C. E. *Biochim. Biophys. Acta* **1990**, *1031*, 143.
(3) Raghuraman, H.; Chattopadhyay, A. *Biosci. Rep.* **2007**, *27*, 189.
(4) Shai, Y. *Trends Biochem. Sci.* **1995**, *20*, 460.
(5) Bello, J.; Bello, H. R.; Granados, E. *Biochemistry* **1982**, *21*, 461.

(6) Raghuraman, H.; Chattopadhyay, A. *Biopolymers* **2006**, *83*, 111.
(7) De Jongh, H. H. J.; Goormaghtigh, E.; Killian, J. A. *Biochemistry* **1994**, *33*, 14521.
(8) Ghosh, A. K.; Rukmini, R.; Chattopadhyay, A. *Biochemistry* **1997**, *36*, 14291.
(9) Raghuraman, H.; Chattopadhyay, A. *Biophys. J.* **2004**, *87*, 2419.
(10) Raghuraman, H.; Chattopadhyay, A. *Biochim. Biophys. Acta* **2004**, *1665*, 29.
(11) Raghuraman, H.; Chattopadhyay, A. *Langmuir* **2003**, *19*, 10332.
(12) Raghuraman, H.; Chattopadhyay, A. *Biophys. J.* **2004**, *33*, 611.
(13) Terwilliger, T. C.; Eisenberg, D. *J. Biol. Chem.* **1982**, *237*, 6016.
(14) Morii, H. S.; Honda, S.; Ohashi, S.; Uedaira, H. *Biopolymers* **1994**, *34*, 481.
(15) Golding, C.; O'Shea, P. *Biochem. Soc. Trans.* **1995**, *23*, 971.
(16) Rabenstein, M.; Shin, Y. K. *Biochemistry* **1995**, *34*, 13390.
(17) Barnham, K. J.; Monks, S. A.; Hinds, M. G.; Azad, A. A.; Norton, R. S. *Biochemistry* **1997**, *36*, 5970.
(18) Cajal, Y.; Jain, M. K. *Biochemistry* **1997**, *36*, 3882.
(19) Bradrick, T. D.; Philippetis, A.; Georghiou, S. *Biophys. J.* **1995**, *69*, 1999.
(20) Oren, Z.; Shai, Y. *Biochemistry* **1997**, *36*, 1826.
(21) Raghuraman, H.; Ganguly, S.; Chattopadhyay, A. *Biophys. Chem.* **2006**, *124*, 115.
(22) Raghuraman, H.; Chattopadhyay, A. *Biophys. J.* **2007**, *92*, 1271.
(23) Lakowicz, J. R. *Principles of Fluorescence Spectroscopy*, 3rd ed.; Springer: New York, 2006.
(24) Dittmer, J. C.; Lester, R. L. *J. Lipid Res.* **1964**, *5*, 126.
(25) McClare, C. W. F. *Anal. Biochem.* **1971**, *39*, 527.
(26) MacDonald, R. C.; MacDonald, R. I.; Menco, B. P.; Takeshita, K.; Subbarao, N. K.; Hu, L. R. *Biochim. Biophys. Acta* **1991**, *1061*, 297.
(27) Abrams, F. S.; London, E. *Biochemistry* **1993**, *32*, 10826.
(28) Kremer, J. M. H.; van der Esker, M. W.; Pathmamanoharan, C.; Wiersema, P. H. *Biochemistry* **1977**, *16*, 3932.
(29) O'Connor, D. V.; Phillips, D. *Time-correlated Single Photon Counting*; Academic Press: London, 1984; pp 180−189.
(30) Lampert, R. A.; Chewter, L. A.; Phillips, D.; O'Connor, D. V.; Roberts, A. J.; Meech, S. R. *Anal. Chem.* **1983**, *55*, 68.
(31) Grinvald, A.; Steinberg, I. Z. *Anal. Biochem.* **1974**, *59*, 583.
(32) Yang, L.; Harroun, T. A.; Weiss, T. M.; Ding, L.; Huang, H. W. *Biophys. J.* **2001**, *81*, 1475.
(33) Ladokhin, A. S.; White, S. H. *J. Mol. Biol.* **1999**, *285*, 1363.
(34) Chattopadhyay, A. *Chem. Phys. Lipids.* **2003**, *122*, 3.
(35) Raghuraman, H.; Kelkar, D. A.; Chattopadhyay, A. In *Reviews in Fluorescence 2005*; Geddes, C. D., Lakowicz, J. R., Eds.; Springer: New York, 2005; pp 199−222.
(36) Demchenko, A. P. *Luminescence* **2002**, *17*, 19.
(37) Bhattacharyya, K. *Acc. Chem. Res.* **2003**, *36*, 95.
(38) Bhattacharyya, K.; Bagchi, B. *J. Phys. Chem. A* **2000**, *104*, 10603.
(39) Haldar, S.; Chattopadhyay, A. *J. Phys. Chem. B* **2007**, *111*, 14436.
(40) Kelkar, D. A.; Chattopadhyay, A. *Biophys. J.* **2005**, *88*, 1070.
(41) We have used the term maximum of fluorescence emission in a somewhat wider sense here. In every case, we have monitored the wavelength corresponding to maximum fluorescence intensity, as well as the center of mass of the fluorescence emission. In most cases, both these methods yielded the same wavelength. In cases where minor discrepancies were found, the center of mass of emission has been reported as the fluorescence maximum.
(42) Hristova, K.; Dempsey, C. E.; White, S. H. *Biophys. J.* **2001**, *80*, 801.
(43) White, S. H.; Wimley, W. C. *Curr. Opin. Struct. Biol.* **1994**, *4*, 79.
(44) Mukherjee, S.; Chattopadhyay, A. *J. Fluoresc.* **1995**, *5*, 237.
(45) Prendergast, F. G. *Curr. Opin. Struct. Biol.* **1991**, *1*, 1054.
(46) Stubbs, C. D.; Meech, S. R.; Lee, A. G.; Phillips, D. *Biochim. Biophys. Acta* **1985**, *815*, 351.
(47) Li, Y.-H.; Chan, L.-M; Tyer, L.; Moody, R. T.; Himel, C. M.; Hercules, D. M. *J. Am. Chem. Soc.* **1975**, *97*, 3118.
(48) Ghiggino, K. P.; Lee, A. G.; Meech, S. R.; O'Connor, D. V.; Phillips, D. *Biochemistry* **1981**, *20*, 5381.
(49) Chattopadhyay, A. In *Biomembrane Structure and Function: The State of the Art*; Gaber, B. P., Easwaran, K. R. K., Eds.; Adenine Press: Schenectady, NY, 1992; pp 153−163.
(50) London, E.; Ladokhin, A. S. In *Current Topics in Membranes*; Benos, D., Simon, S., Eds.; Elsevier: San Diego, CA, 2002; pp 89−115.
(51) Chattopadhyay, A.; London, E. *Biochemistry* **1987**, *26*, 39.
(52) Seliskar, C. J.; Brand, L. *J. Am. Chem. Soc.* **1971**, *93*, 5414.
(53) Lakowicz, J. R.; Gryczynski, I.; Laczko, G.; Wiczk, W.; Johnson, M. L. *Protein Sci.* **1994**, *3*, 628.
(54) Sengupta, D.; Meinhold, L.; Langosch, D.; Ullmann, G. M.; Smith, J. C. *Proteins.* **2005**, *58*, 913.
(55) Bachar, M.; Becker, O. M. *Biophys. J.* **2000**, *78*, 1359.
(56) Toraya, S.; Katsuyuki, N.; Naito, A. *Biophys. J.* **2004**, *87*, 3323.
(57) Chen, X.; Wang, J.; Boughton, A. P.; Kristalyn, C. B.; Chen, Z. *J. Am. Chem. Soc.* **2007**, *129*, 1420.
(58) Vogel, H. *Biochemistry* **1987**, *26*, 4562.
(59) Wall, J.; Golding, C. A.; Van Veen, M.; O'Shea, P. *Mol. Membr. Biol.* **1995**, *12*, 183.
(60) Bernèche, S.; Nina, M.; Roux, B. *Biophys. J.* **1998**, *75*, 1603.
(61) Castano, S.; Cornut, I.; Buttner, K.; Dasseux, J. L.; Dufourcq, J. *Biochim. Biophys. Acta* **1999**, *1416*, 161.

JP805299G